

Creep and creep–fatigue crack growth

Ashok Saxena

Received: 28 November 2014 / Accepted: 24 January 2015 / Published online: 17 February 2015
© The Author(s) 2015. This article is published with open access at Springerlink.com

Abstract Creep and creep–fatigue considerations are important in predicting the remaining life and safe inspection intervals as part of maintenance programs for components operating in harsh, high temperature environments. Time-dependent deformation associated with creep alters the crack tip stress fields established as part of initial loading which must be addressed in any viable theory to account for creep in the vicinity of crack tips. This paper presents a critical assessment of the current state-of-the-art of time-dependent fracture mechanics (TDFM) concepts, test techniques, and applications and describes these important developments that have occurred over the past three decades. It is concluded that while big advances have been made in TDFM, the capabilities to address some significant problems still remain unresolved. These include (a) elevated temperature crack growth in creep-brittle materials used in gas turbines but now also finding increasing use in advanced power-plant components (b) in predicting crack growth in weldments that inherently have cracks or crack-like defects in regions with microstructural gradients (c) in development of a better fundamental understanding of creep–fatigue–environment interactions, and (d) in prognostics of high temperature

component reliability. It is also argued that while these problems were considered intractable a few years ago, the advances in technology do make it possible to systematically address them now and advance TDFM to its next level in addressing the more difficult but real engineering problems.

Keywords Cracks · Fatigue · Creep · Welds · Ni-base alloys · Ferritic steels · C_t parameter · C^* -integral · $(C_t)_{avg}$ parameter

1 Introduction

Structural components that experience harsh environments such as high temperatures and stresses are common in land-based steam and gas turbines, in aircraft engines, and in power-plant components. These components are often cast, forged or welded making them prone to having crack-like manufacturing defects. The considerations that are involved in determining the risk of fracture in these components are several that include:

- Transient and steady-state thermal stresses
- Hold times, static and cyclic stresses due to external loading
- Environmental effects
- Creep deformation (primary, secondary, tertiary creep) and rupture
- Creep–fatigue and environmental damage mechanisms

A. Saxena (✉)
College of Engineering, University of Arkansas, 130 A
John A. White Hall, 790 W. Dickson Street, Fayetteville,
AR 72701, USA
e-mail: asaxena@uark.edu

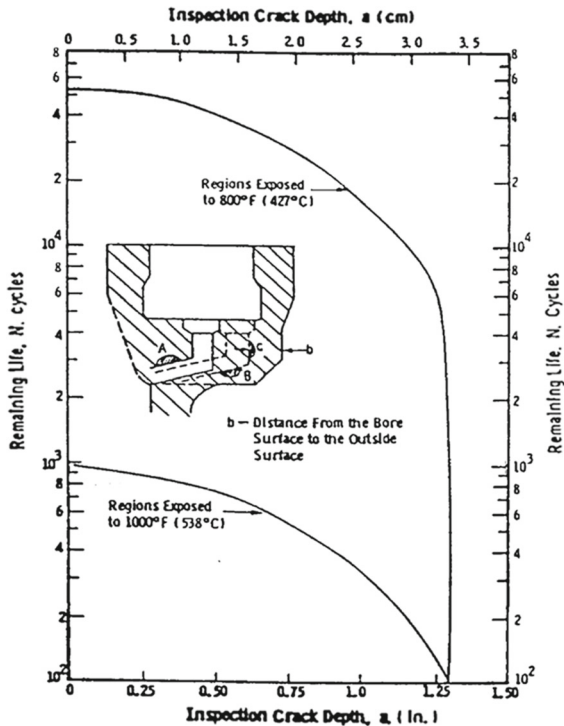


Fig. 1 The estimated relationship between flaw size at inspection and the remaining life in steam turbine casings in regions exposed to different temperatures (Saxena et al. 1986)

- Varying material properties due to temperature gradients
- Complex crack geometries and variable amplitude loading
- In-service degradation of material properties
- Weldments with microstructural gradients
- Directionally solidified and single crystal materials with anisotropic creep and plastic deformation properties

Such a set of complex conditions are difficult to address in a single comprehensive theory so researchers have endeavored to break-up the problem into smaller elements and address them one or two at a time. This has led to a comprehensive set of analytical tools and models that allow us to approach real problems using the most appropriate analytical tools for specific situations. Examples of such analyses date back to nineteen eighties in the form of remaining life and inspection interval calculations in steam turbine casings used in ships to generate the auxiliary power as shown in Fig. 1 (Saxena et al. 1986). For regions exposed to 538 °C (1,000 °F), and a crack depth of 6 mm (0.25 in.) in the steam

passage-ways of steam turbine casings, the estimated remaining life was 800 cycles or at 50 cycles/year, about 16 years. In this example the crack growth rates estimated from direct measurements of oxide thickness on crack surfaces excavated from turbine casings validated the analytical estimates thus, significantly raising the confidence levels in the models that were developed specifically for this application.

1.1 Early developments in TDFM

Some of the earliest studies involving the use of fracture mechanics to predict crack growth rates at elevated temperatures are in the work of James (1972) who successfully extended the idea of using the cyclic stress intensity parameter, ΔK , to correlate fatigue crack growth behavior of 304 stainless steel at elevated temperatures at various frequencies. About the same time, Siverns and Price (1973) unsuccessfully attempted to correlate creep crack growth rate to the stress intensity parameter, K . Under static loading, K uniquely characterizes the crack tip stress field only upon loading at time, $t = 0^+$. With elapse of time, stress relaxation at the crack tip occurs due to creep deformation and there is no longer a uniqueness in the relationship between K and the crack tip stress fields (Saxena 1980; Riedel and Rice 1980). On the other hand under cyclic loading, the fatigue crack growth rate does continue to be uniquely characterized by ΔK but only if the time related parameters such as the frequency of loading and the loading waveform are kept constant (Saxena 1980; Saxena et al. 1981; Riedel 1983). The functional relationship between fatigue crack growth rate and ΔK is given by Eq. 1.

$$\frac{da}{dN} = f(\Delta K, \text{frequency}, \text{waveform}, R, T) \quad (1)$$

where, da/dN = fatigue crack growth rate and R = load ratio of the loading waveform and T = test temperature.

Landes and Begley (1976) proposed the C^* -integral for characterizing creep crack growth rates, based on the mathematical analogy between C^* and Rice's J -integral (Rice 1968), as a candidate parameter for characterizing creep crack growth rate. They also recognized its importance as a crack tip parameter capable of uniquely characterizing the crack tip stress fields (Eq. 2a) under the idealized conditions of widespread secondary-stage creep throughout the cracked

body by making another analogy to the HRR fields proposed for J-Integral (Hutchinson 1968; Rice and Rosengren 1968). C^* was also related to the stress-power dissipation rate (U^*) in their paper as shown in Eq. (2b). They attempted to experimentally demonstrate the validity of C^* by conducting experiments on alloy A286 using both dominantly bend-type, compact, C(T), specimens and middle crack tension, M(T), specimens. Their results only met with partial success because the condition of widespread secondary creep was not met in their specimens for much of the duration of the tests. Consequently, the creep crack growth rates measured from C(T) and M(T) specimens differed from each other. Attempts to find J-like parameters to correlate creep crack growth rates were also made in Europe (Nikbin et al. 1976) and in Japan (Taira et al. 1979) but the association with crack tip stress fields was not recognized in these studies. Saxena (1980) showed that creep crack growth rates were uniquely correlated with C^* -Integral for C(T) and M(T) specimens for 304 stainless steel at 594 °C (1,100 °F) because the necessary conditions of widespread steady-state creep (a term interchangeably used with secondary creep in the literature and here) were established shortly after loading and the creep crack growth rate occurred primarily under this tailor-made conditions for C^* to describe the crack tip conditions. In the same paper it was also shown how the value of C^* -Integral can be analytically calculated from equations derived to estimate J -Integral for cracked bodies under fully plastic conditions such as in Kumar et al. (1981).

$$\sigma_{ij} = \left(\frac{C^*}{I_n A r} \right)^{\frac{1}{n+1}} \hat{\sigma}_{ij}(\theta, n) \tag{2a}$$

$$C^* = -\frac{1}{B} \frac{dU^*}{da} \tag{2b}$$

where, A and n are steady-state creep constants in a Norton’s power–law relationship, r = distance from the crack tip, θ is the angular coordinate, $\hat{\sigma}_{ij}(\theta, n)$ is an angular function tabulated with the HRR fields, B is thickness of the planar cracked body and a is the crack size.

2 Stress analysis of cracks in the small-scale-creep regime

With establishment of C^* as the crack tip parameter for characterizing creep crack growth rates under

widespread steady-state creep conditions, the attention in early nineteen eighties turned to its limitations and search for parameters that could be used under small-scale creep conditions and would become identical to C^* when widespread steady-state creep conditions are established. This body of analytical and numerical simulations work can be divided in two parts (a) consideration of stationery cracks and (b) consideration of moving cracks.

2.1 Analysis of stationery cracks

Work of Riedel and Rice (1980), Ohji et al. (1979) and Bassani and McClintock (1981) was key in unlocking the mechanics of this problem. The Riedel and Rice and Ohji et al. analytically derived the crack tip stress fields ahead of the crack tip under small-scale creep conditions while Bassani and McClintock (1981) numerically verified these analytical results and extended the analysis by proposing a parameter, $C(t)$, that characterized the amplitude of the crack tip stress singularity from small-scale creep all the way to widespread creep for steady-state creep deformation, Eq. 3. For widespread creep, $C(t)$ becomes identical to C^* and for small scale creep it is related to a line integral that is path dependent given in Eq. 4.

$$\sigma_{ij} = \left(\frac{C(t)}{I_n A r} \right)^{\frac{1}{n+1}} \hat{\sigma}_{ij}(\theta, n) \tag{3}$$

For small-scale creep,

$$C(t) = \int_{\Gamma \rightarrow 0} \left[W^* \sin \theta - T_i \left(\frac{\partial \dot{u}_i}{\partial x_1} \right) \right] ds \tag{4}$$

where, \mathbf{T} is the traction vector, W^* is the stress-power density and \mathbf{u} is the displacement vector, Γ is a contour that begins on the lower crack surface and travels counter clock-wise ending on the upper crack surface. The contour must be defined in a region where creep deformation dominates near the crack tip and thus the condition $\Gamma \rightarrow 0$. Under widespread creep, $C(t)$ becomes identical to C^* by definition. Schemes were developed (Bassani and McClintock 1981) to estimate $C(t)$ analytically and the following equations were proposed.

$$\text{For } t \ll t_1, \quad C(t) \approx \frac{K^2(1 - \nu^2)}{EA(n + 1)t} \tag{5a}$$

$$\text{For } t \gg t_1, \quad C(t) = C^* \quad (5b)$$

$$\text{For } 0 < \frac{t}{t_1} < \infty,$$

$$C(t) \approx C^* \left[\frac{K^2(1-\nu^2)}{EA(n+1)t} + 1 \right] \quad (5c)$$

The transition time, t_1 , between small-scale creep and widespread creep was obtained by equating Eqs. 5a and 5b for the two extreme conditions to derive Eq. 6: (Riedel and Rice 1980; Ohji et al. 1979).

$$t_1 = \frac{K^2(1-\nu^2)}{EA(n+1)C^*} \quad (6)$$

Based on Eqs. 3 and 5a, b, c, $C(t)$ is an attractive parameter for characterizing creep crack growth rate but its major disadvantage is that it cannot be measured at the loading pins or it is not uniquely related to the stress-power dissipation rate in the small-scale creep regime like C^* is in the widespread creep regime. Recall that C^* serves both functions. The former shortcoming is particularly a problem because one is then completely dependent on accurate constitutive equations for estimating $C(t)$ which must include, in addition to elastic deformation and steady-state creep, the effects of instantaneous plasticity, primary creep, tertiary creep, 2-D versus 3-D stress fields in the crack tip region and the scale of creep deformation. All these deformation phenomena are operative in the crack tip region so it is not sufficient to just account for elastic deformation and steady-state creep as is assumed in Eqs. (5).

Addressing the above shortcoming, Saxena (1986) proposed the C_t parameter, measurable at the load-line of the cracked body and thus including contributions from all the different deformation mechanisms present at the crack tip. C_t generalizes the stress-power dissipation rate definition of C^* into the small-scale creep regime in the following way:

$$(C_t)_{ssc} = -\frac{1}{B} \frac{\partial U_t^*(a, t, \dot{V}_c)}{\partial a} \quad (7)$$

where, U_t^* is the instantaneous stress-power at any time, t , that is also a function of the crack size, a , and the deflection rate due to creep, \dot{V}_c . Expressions were derived to measure the value of $(C_t)_{ssc}$ in specimens (Saxena 1986), Eq. (8), and subsequently it was also uniquely related to the rate of expansion of the creep zone at the crack tip (Bassani et al. 1989), Eq. (9).

$$(C_t)_{ssc} = \frac{P \dot{V}_c F'}{BW F} \quad (8)$$

$$(C_t)_{ssc} = \frac{2K^2(1-\nu^2) F'}{EW F} \beta \dot{r}_c \quad (9)$$

where, W = width of the cracked body, E = elastic modulus, $\beta \approx \frac{1}{3}$, P = Load on the specimen, ν = Poisson's ratio, $F = K$ -calibration factor = $\left(\frac{K}{P}\right) BW^{\frac{1}{2}}$, $F' = dF/d\left(\frac{a}{W}\right)$, \dot{r}_c = rate of expansion of the creep zone size at the crack tip. C_t also then uniquely characterizes the rate of expansion of the creep zone size and is therefore an attractive candidate crack tip parameter and it is also by definition identical to C^* under widespread creep conditions. However, under small-scale creep conditions $C_t \neq C(t)$ (Saxena 1998).

2.2 Growing crack considerations in creep-ductile and creep-brittle materials

The growing cracks perturb the stationary crack fields and if this perturbation occurs over a sizeable region near the crack tip compared to the region of dominance of the stationary crack tip fields, crack parameters such as K , C^* and C_t may be unable to correlate uniquely with creep crack growth rates. The material characteristics themselves play a big role in determining which of the above parameters, if any, are appropriate. Thus, a classification of the different material types is in order.

High temperature structural materials may be classified as creep-ductile or creep-brittle materials. Creep-ductile materials are ones in which the crack growth is accompanied by substantial amounts of time-dependent creep strains and the region of influence of growing crack fields is small in comparison to the creep zone size. Similarly, in the case of widespread creep, the region of influence of growing crack fields are small in comparison to the zone in which C^* dominates the crack tip fields. Examples of these materials are chromium (Cr), Molybdenum (Mo) and vanadium (V) containing ferritic or bainitic steels used in the fossil power-plant applications. Creep-brittle materials, on the other hand, are those in which creep crack growth occurs in the presence of small amounts of creep deformation so the creep zone size ahead of the moving crack tip always remains constrained within a small region. This class of materials includes Nickel base superalloys used commonly in the land-based gas turbines and in aero-engines and are now finding usage

in advanced power-plant components and in advanced nuclear power stations.

Hui and Riedel (1981), Reidel and Wagner (1981), Hui (1983, 1986) proposed that in order for steady-state crack growth conditions characterized by K and C^* to exist, both the crack growth rate and the magnitude of crack tip parameters must change slowly with time. These conditions are expressed by Eqs. (10) and (11) for the conditions of small-scale creep dominated by K and widespread creep dominated by C^* , respectively. The dots signify time derivatives of those quantities.

$$|\ddot{a}| \leq \left[\frac{\dot{a}^{n-2}}{EAK^{n-1}} \right]^{\frac{2}{n-3}} \tag{10a}$$

$$|\dot{K}| \leq \left[\frac{\dot{a}^{n-1}}{E^2A^2K^{n+1}} \right]^{\frac{1}{n-3}} \tag{10b}$$

$$|\ddot{a}| \leq A \left(\frac{E^{n+1}C^{*n-1}}{\dot{a}^{n-3}} \right)^{1/2} \tag{11a}$$

$$|\dot{C}^*| \leq A \left(\frac{(EC^*)^{n+1}}{\dot{a}^{n-1}} \right)^{1/2} \tag{11b}$$

Conditions bound by Eqs. (10) and (11) under which steady-state creep crack growth uniquely characterized either by K or C^* may not frequently be encountered in practice. Therefore, it is also important to understand the crack tip mechanics during transient periods which may account for a significant portion of the crack growth during a laboratory test or in a component.

Transient regions are defined as (a) the region prior to the establishment of C^* dominated crack tip conditions for cracks growing at speeds slow enough to be considered stationery for practical purposes such as in creep-ductile materials or (b) the region in which cracks grow at sufficient speeds in creep-resistant or creep-brittle materials to preclude C^* or C_t dominated conditions but also steady-state conditions dominated uniquely by the stress intensity parameter, K , are not achieved. It may take substantial amounts of crack extension prior to the rates being uniquely correlated to K .

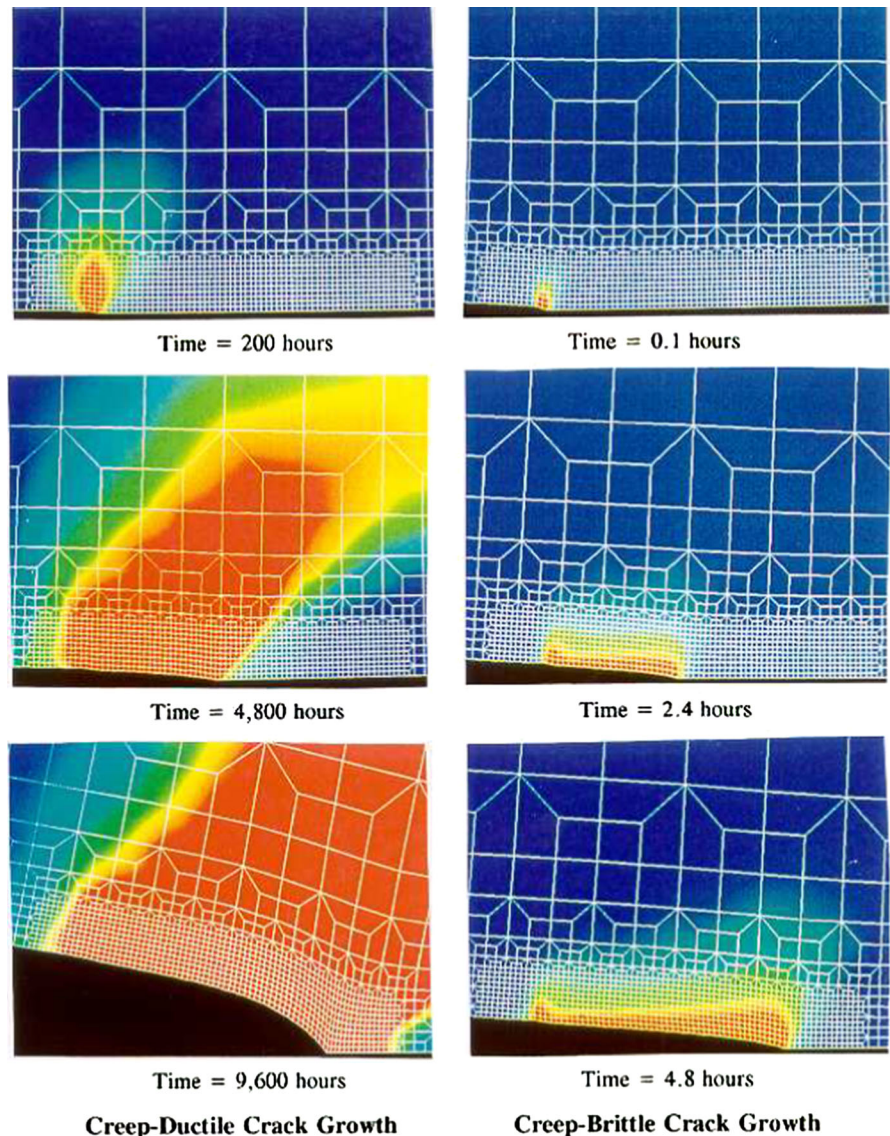
Figure 2 shows the results of finite element simulations that were carried out by Hall et al. (1997) to understand the development of the crack tip creep deformation with time in real tests conducted on a creep-resistant aluminum alloy. These simulations were carried out on C(T) specimens used in actual tests in which

the creep deformation properties, the specimen geometry and the load levels were identical in two separate simulations. In one case the crack size versus time history input into the simulations were the experimentally measured crack size with time. These conditions were typical of creep-brittle materials. In the other case, the crack growth rates were artificially decreased by a factor of ten to allow more creep strains to accumulate at the crack tip. These conditions are characteristic of creep-ductile materials. The crack tip creep zone evolution is shown to be strongly influenced by the crack growth rate and the creep zone size and shape are quite different for the two cases as evident from Fig. 2. Also in the creep-brittle case, the creep zone shape ahead of the moving crack tip changes with time and therefore, steady-state conditions cannot develop during the tests and K is not expected to uniquely characterize the creep crack growth rates that was in fact experienced as shown in Fig. 3 (Hamilton et al. 1997) where every test produced a different correlation between creep crack growth rate and K .

In creep-ductile materials, the extent of the region in which the growing crack field is dominant is negligible and the creep zone size evolves from small-scale to widespread creep conditions giving rise to transient crack tip conditions (Saxena 1986). The creep crack growth rates have been shown in such instances to uniquely correlate with the C_t parameter (Saxena 1986 and Saxena et al. 1994) as seen in Fig. 4. In these tests conducted on C(T) specimens that were 254 mm wide, it was shown that very significant amounts of crack extension occurred prior to the establishment of widespread creep conditions and in spite of that, all creep crack growth rate data correlated well with C_t . Thus, we conclude that our understanding of creep crack growth in creep-ductile materials under a wide range of transient and steady-state conditions is good but not so for creep-brittle materials for which there does not exist a C_t type parameter.

To distinguish between creep-ductile and creep-brittle materials, Saxena et al. (1983) proposed a method based on partitioning the measured load-line displacement rate, \dot{V} , during testing between that associated with creep deformation (\dot{V}_c) for no crack growth and that due to change in elastic (\dot{V}_e) and plastic (\dot{V}_p) compliance of the specimen due to crack extension. The measured load-line displacement rate (\dot{V}) is the sum of all three. For steady-state creep crack growth to occur that is correlated with either C^* or C_t , $\dot{V}_c \gg (\dot{V}_e + \dot{V}_p)$.

Fig. 2 Finite element simulations of creep crack growth under creep-ductile and creep-brittle conditions Hall et al. (1997). The specimens analyzed were C(T) type with a width of 50.8 mm and a starting crack size of 20.3 mm



They estimated the value of $\dot{V}_e + \dot{V}_p$ by Eq. 12:

$$\dot{V}_e + \dot{V}_p \approx \frac{\dot{a}B}{p} \left[\frac{2k^2}{E} + (m+1)J_p \right] \quad (12)$$

where, J_p is the fully plastic component of the J -integral and m is the plastic exponent in the power-law relationship between plastic strain and applied stress for the material. It is required that for creep crack growth rate to correlate with C_t , that $\dot{V}_c \gg (\dot{V}_e + \dot{V}_p)$. In practice, the condition is expressed as $\dot{V}_c \geq 0.8\dot{V}$.

Standard test methods for characterizing creep crack growth rates in creep-ductile materials are available

via the American Society for Testing and Materials (ASTM) test standard E1457 [ASTM Standard E1457]. This method currently only applies to creep-ductile materials for which accepted crack tip parameters are available to correlate the creep crack growth behavior. In the future, it would be useful to develop these methods to include creep-brittle materials also.

2.3 Consideration of primary creep

A creep constitutive law which combines elastic deformation, primary creep, and steady-state creep can be written as in Eq. 13.

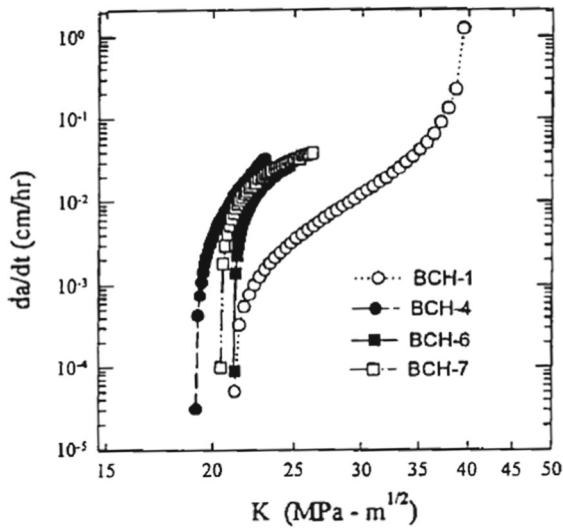


Fig. 3 Creep crack growth behavior of a creep-brittle Al alloy 2519-T87 (Hamilton et al. 1997). The lack of uniqueness in the correlation between da/dt and K is apparent in data from various specimens that are identical except in the starting crack size and the applied load

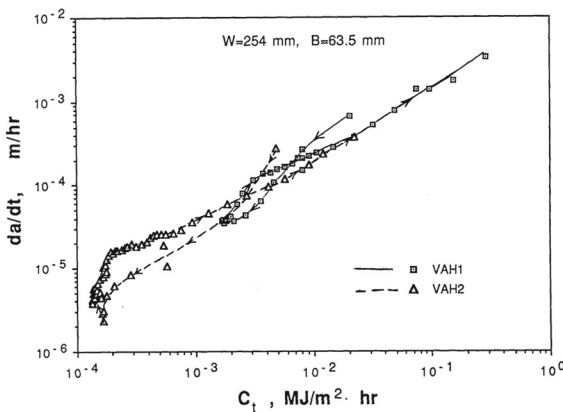


Fig. 4 Creep crack growth rate as a function of C_I parameter in 1Cr-1Mo-0.25V steel at 538 °C under small-scale creep to widespread creep in large C(T) specimens (Saxena et al. 1994). VAH1 and VAH 2 refer to two specimens tested at different load levels and the arrows point to crack growth rates from the beginning of the test going forward in time

$$\dot{\epsilon} = \frac{\dot{\sigma}}{E} + A_1 \epsilon^{-p} \sigma^{n_1(1+p)} + A \sigma^n \tag{13}$$

In Eq. 13, the first and the third terms on the right hand side of the equation pertain to elastic and secondary creep strains while the middle term pertains to primary creep strains that contain three constants, A_1 , n_1 , and p that are obtained from regression of pri-

mary creep data. If primary creep condition dominates the deformation behavior, Eq. 13 can be simplified to Eqs. 14a, b, c.

$$\dot{\epsilon} = A_1 \epsilon^{-p} \sigma^{n_1(1+p)} \tag{14a}$$

or

$$\epsilon = [(1 + p) A_1 t]^{1/(1+p)} \sigma^{n_1} \tag{14b}$$

and

$$\dot{\epsilon} = A_1 [(1 + p) A_1 t]^{-\frac{p}{1+p}} \sigma^{n_1} \tag{14c}$$

Riedel (1981) recognized that Eq. 14b for constant time is analogous to power-law relationship between stress and strain, thus, a J -integral can be defined that will be path-independent for any given time t . He also pointed to another path-independent integral, C_h^* which is independent of time for primary creep conditions as in Eq. 15.

$$J = C_h^* t^{\frac{1}{1+p}} \tag{15}$$

C_h^* can be obtained by replacing A by $[(1 + p) A_1 t]^{1/(1+p)}$ and n by n_1 in equations for determining C^* . Further, from Eq. 14c, C^* -integral can also be derived that is a function of time and related to C_h^* by Eq. 16.

$$C^*(t) = \frac{C_h^*}{(1 + p)t^{\frac{p}{1+p}}} \tag{16}$$

These equations permit accounting for primary creep, if present, in estimating the magnitude of crack tip parameters. This approach can also be extended for small-scale creep. For further details, the readers are referred to Saxena (1998).

This section shows that the crack tip mechanics for stationary cracks under a variety of crack tip deformation conditions is well understood. For creep-ductile materials where the rate of advance of the crack tip is much slower than the rate of creep deformation at the crack tip, this understanding is sufficient for the purposes of analyzing components. In creep-brittle materials, where there is competition between the evolution of stress and strain fields due to time-dependent deformation and due to crack growth, there are no unifying concepts that are currently available to analyze these situations. This is a major gap in technology that currently exists and prevents the use of time-dependent fracture mechanics approach to an important class of

high temperature materials such as intermetallics and Ni base alloys and high temperature ceramics. This can be addressed with more research.

3 Creep-fatigue crack growth

3.1 Crack tip parameters for creep-fatigue loading

For cyclic loading, the crack tip stress fields during each cycle will at least partially regenerate every cycle if small-scale creep and small-scale plastic deformation can be maintained. Thus even in the presence of a hold time that follows the rising load portion of the waveform, crack growth rates can be uniquely characterized by ΔK for that loading waveform and cycle time. If either the cycle time or loading waveform changes, the functional relationship between the crack growth rate per cycle, da/dN , and ΔK will change. This was earlier expressed in Eq. 1.

Some examples of such correlations are shown in Figs. 5 and 6 for creep-ductile and creep-brittle materials. These relationships are valid only for time periods of cycles that are much less than the transition time defined in Eq. 6. For longer times, the validity of the small-scale-creep conditions cannot be assured so the

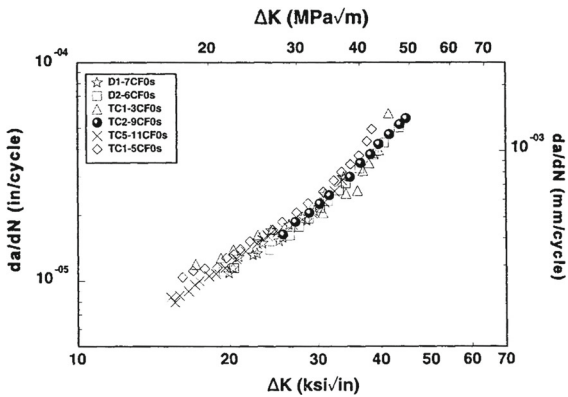
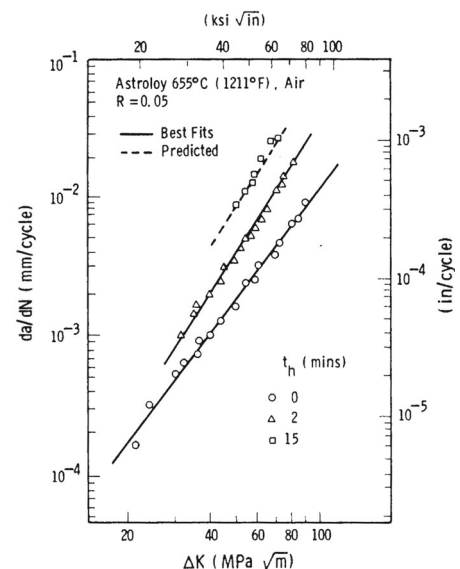
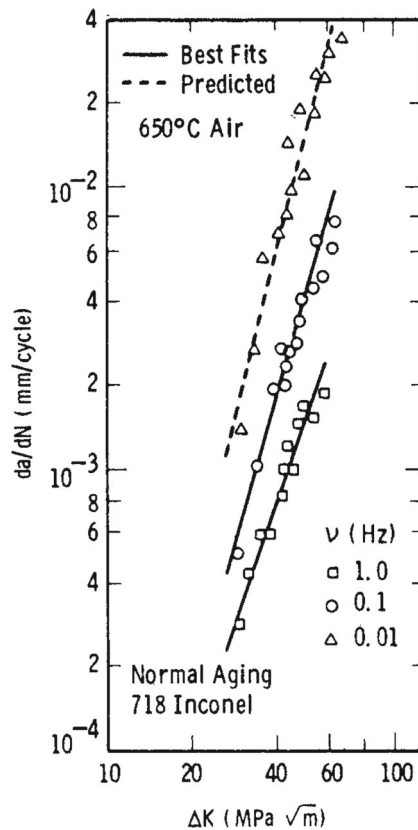


Fig. 5 Fatigue crack growth behavior at of a 1Cr-1Mo-0.25V alloy at 538 °C (Grover 1997; Grover and Saxena 1999). The data are a collection of results from samples taken from base metal (D1 and D2) and from weldments (TC1, TC2, and TC-5)

Fig. 6 a Fatigue crack growth behavior of Inconel 718 at various loading frequencies (Floreen and Kane 1980) and **b** for various hold times for Astroloy (Pelloux and Huang 1980)



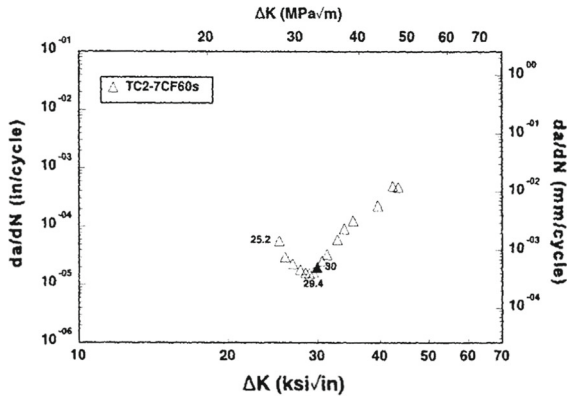


Fig. 7 Fatigue crack growth rate in a Cr–Mo–V creep-ductile steel at 5,380 °C for a waveform containing a hold time of 60 s at the maximum load (Grover and Saxena 1995)

validity of Eq. 1 also comes into question. In Fig. 5, results are presented from multiple tests on a creep-ductile 1 Cr–1Mo–0.25V steel at 538 °C at a loading frequency of 1 Hz subjected to continuous cycling using a triangular waveform at different load amplitudes (Grover 1997; Grover and Saxena 1999). All tests yield identical crack growth rates when correlated with ΔK . In Fig. 6, the loading frequency is varied for tests

Studies (Grover and Saxena 1999; Yoon et al. 1993) performed on creep-ductile power plant materials using C(T) specimens have shown $(C_t)_{avg}$ to be the most effective crack tip parameter in correlating creep-fatigue crack growth rates under trapezoidal wave form with a hold time, t_h . In such cases, the time dependent crack growth, $(da/dt)_{avg}$, during the hold period is expressed as a function of the average magnitude of the C_t parameter, $(C_t)_{avg}$, defined in Eq. 17.

$$(C_t)_{avg} = \frac{1}{t_h} \int_0^{t_h} C_t dt \tag{17}$$

$(C_t)_{avg}$ is estimated from Eq. 18 for test specimens in which both load and load-line deflection behavior with time are measured:

$$(C_t)_{avg} = \frac{\Delta P \Delta V_c}{(BB_N)^{1/2} W t_h} (F'/F) \tag{18}$$

where, ΔP is the applied load range, ΔV_c is the difference in load-line displacement between the end and start of the hold time, t_h , during a cycle. F'/F is given by Eq. 19.

$$\frac{F'}{F} = \left[\left(\frac{1}{2 + a/W} \right) + \left(\frac{3}{2(1 - a/W)} \right) \right] + \left[\frac{(4.64 - 26.64(a/W) + 44.16(a/W)^2 - 22.4(a/W)^3)}{0.886 + 4.64(a/W) - 13.32(a/W)^2 + 14.72(a/W)^3 - 5.6(a/W)^4} \right] \tag{19}$$

conducted on a creep-brittle Inconel 718 (Floreen and Kane 1980) and Astroloy (Pelloux and Huang 1980) materials. We see a clear layering of the data with different loading frequencies or hold times validating Eq. 1. The cyclic crack growth rates show a definite trend with increasing hold time or increasing cycle time but still show a good correlation with ΔK .

When hold time is added to the cyclic loading waveforms of creep-ductile materials, the fatigue crack growth rates tend to show a hook in the behavior when correlated to ΔK , Fig. 7 (Grover and Saxena 1995). This behavior is due to ratcheting of the minimum load-line deflection with each cycle because the specimen accumulates creep strains near the crack tip that are not fully reversed during unloading. For such situations, the use of the $(C_t)_{avg}$ parameter defined by Saxena and Gieseke (1987) is recommended.

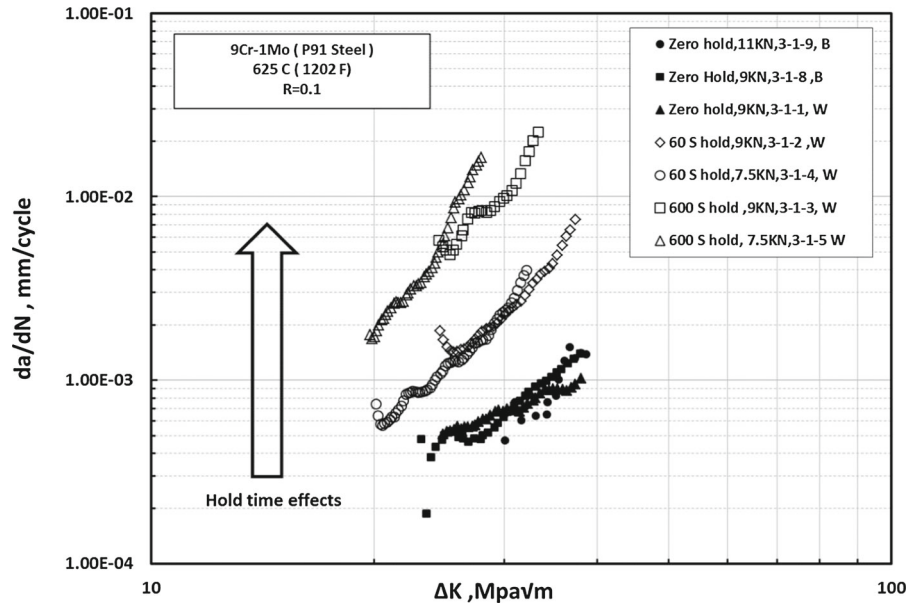
The value of $(C_t)_{avg}$ from Eq. 18 is appropriate for the small scale creep regime. When hold times are too small for reliable measurement of load-line displacement range because of the resolution limitations of the extensometer, $(C_t)_{avg}$ can be estimated using Eq. 20 (Yoon et al. 1992).

$$(C_t)_{avg} = (C_t)_{ssc} + C^* \tag{20}$$

$(C_t)_{ssc}$ can be estimated using Eq. 21 (Saxena and Gieseke 1987):

$$(C_t)_{ssc} = \frac{2\alpha\beta(1 - \nu^2)}{E} F_{cr}(\theta, n) \frac{\Delta K^4}{W} (F'/F) (EA)^{\frac{2}{n-1}} t_h^{-\frac{n-3}{n-1}} \tag{21}$$

Fig. 8 Fatigue crack growth rate behavior of 9Cr-1Mo steel at 625 °C as a function of ΔK (Narasimhachary and Saxena 2013)



where

$$\alpha = \frac{1}{2\pi} \left(\frac{(n+1)^2}{1.38n} \right)^{\frac{2}{n-1}} \quad (22)$$

For $\theta = 90^\circ$, the value of $\beta \approx 0.33$ and $F_{cr}(90^\circ, 8.24) = 0.387$ (Saxena and Gieseke 1987). C^* can be estimated using Eq. 23

$$C^* = A(W-a)h_1(a/W, n) \left(\frac{P}{1.455\eta_1 B(W-a)} \right)^{n+1} \quad (23)$$

where, η_1 for C(T) specimen is given by Eq. 24.

$$\eta_1 = \left[\left(\frac{2a}{W-a} \right)^2 + 2 \left(\frac{2a}{W-a} \right) + 2 \right]^{1/2} - \left[\left(\frac{2a}{W-a} \right) + 1 \right] \quad (24)$$

The first term on the right hand side of the Eq. (21) represents the small-scale creep contribution and second term represents the extensive creep contribution to the value of $(C_t)_{avg}$. The function $h_1(a/W, n)$ for various a/W and n are available in Kumar et al. (1981).

The fatigue crack growth rates, da/dN , are plotted as a function of ΔK , as shown in Fig. 8 (Narasimhachary and Saxena 2013). The data with hold times of 60 and 600 s do not uniquely correlate with ΔK even between

tests performed at the same hold times, during the initial portions of the tests. There is also a significant contribution of time dependent crack growth under both hold time conditions signaling creep-fatigue interactions being present. These data were next plotted with the $(C_t)_{avg}$ parameter.

The average time-dependent crack growth rates, $(da/dt)_{avg}$, were calculated using both the linear damage summation model and the dominant damage model. The governing equation for the linear damage summation model under creep-fatigue condition is given by Eq. 25.

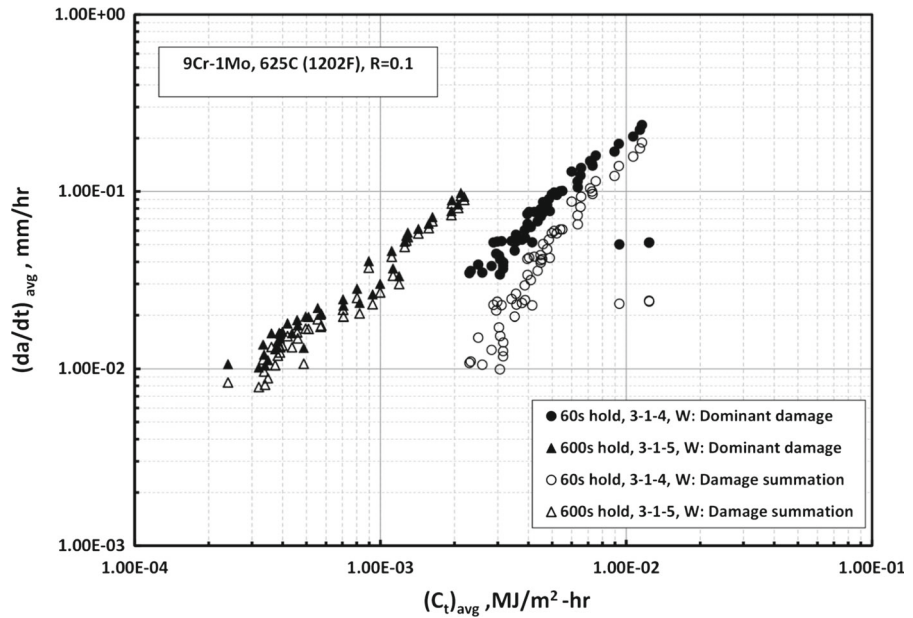
$$\frac{da}{dN} = \left(\frac{da}{dN} \right)_{cycle} + \left(\frac{da}{dN} \right)_{time} \quad (25)$$

where $(da/dN)_{time}$ is related to $(da/dt)_{avg}$ by:

$$\left(\frac{da}{dt} \right)_{avg} = \frac{1}{t_h} \left(\frac{da}{dN} \right)_{time} \quad (26)$$

The first term on the right hand side of the Eq. 25 accounts for cycle dependent crack growth rate and the second term represents the time-dependent part. In this approach, the cycle-dependent and the time-dependent crack growth rates during creep-fatigue conditions are assumed to be independently additive. The cycle-dependent crack growth rate $(da/dN)_{cycle}$ was determined from fatigue tests at 625 °C without hold time.

Fig. 9 Average time rate of crack growth during hold-time as a function $(C_t)_{avg}$ of for hold times of 60 and 600 s for 9Cr–1Mo steel at 625 °C (Narasimhachary and Saxena 2013)



By re-arranging the equation, $(da/dt)_{avg}$, can be calculated by Eq. 27.

$$\left(\frac{da}{dt}\right)_{avg} = \frac{1}{t_h} \left[\left(\frac{da}{dN}\right) - \left(\frac{da}{dN}\right)_{cycle} \right] \tag{27}$$

The alternate approach for representing creep–fatigue crack growth is the dominant damage hypothesis. The governing equations for estimating the crack growth rate from this model is given by Eq. 28.

$$\frac{da}{dN} = \max \left[\left(\frac{da}{dN}\right)_{cycle}, \left(\frac{da}{dN}\right)_{time} \right] \tag{28}$$

where $(da/dt)_{avg}$ is expressed by Eq. 29.

$$\left(\frac{da}{dt}\right)_{avg} = \frac{1}{t_h} \left(\frac{da}{dN}\right)_{time} \tag{29}$$

In this approach, the cycle-dependent and the time-dependent crack growth rates during creep–fatigue conditions are assumed to be competing mechanisms and the crack growth rate is determined by the greater of the two. Both approaches, in other words, the dominant damage hypothesis and the damage summation hypothesis, are used to plot the data so that the differences between the two approaches can be assessed.

Figure 9 shows the plot between the average crack growth rates estimated from Eqs. (27) and (29) correlated with $(C_t)_{avg}$ (Narasimhachary and Saxena 2013). The differences in the crack growth behavior for both 60 and 600 s hold times from the linear damage summation and the dominant damage hypothesis are small. Neither of the two approaches addresses true interaction between creep and fatigue but they bound the extent of the interactions between two extremes which is useful in engineering applications. The first approach supposes no interaction while the other supposes that all the crack growth is associated with only one of the two mechanisms. Thus, a conservative way to account for creep–fatigue interactions is to use Eq. 28 for analyzing creep–fatigue crack growth data because it is conservative and then use Eq. 25 in applications when creep–fatigue crack growth rates are being predicted in components.

Another observation from Fig. 9 is the difference in the creep–fatigue crack growth rates between 60 and 600 s hold time in the 9Cr ferritic/martensitic steels. In previous studies involving lower Cr content steels, the data for hold times ranging from 10 s to 24 h follows the same trend when correlated with $(C_t)_{avg}$ (Yoon et al. 1993; Saxena and Gieseke 1987) and all fall within the scatter-band for the creep crack growth behavior. It should be expected that for long hold times, even for the 9Cr material tested in this study, the time-rate of crack growth must converge with the creep crack

growth rates. When creep–fatigue crack growth rates become identical to creep crack growth rates and how that varies from material to material, deserves a more in-depth investigation.

3.2 Creep–fatigue–environment interactions

Several models for creep–fatigue interactions (Saxena et al. 1981; Saxena and Bassani 1984) and for creep–fatigue–environment interactions (Saxena 1983) to account for hold time effects have been proposed. Predictions from these earlier phenomenological models are shown in Fig. 6b in which the data from 0 and 2 min hold-time tests are used to derive the model constants and then the resulting equation is used to predict the expected creep–fatigue–environment dominated crack growth rates for 15 min hold time tests. The figure shows the good agreement between the model prediction and the test results.

A new crack growth model for creep–fatigue environment effects was developed by Evans and Saxena (2009) incorporating a thermally activated dislocation model of Yokobori et al. (1975) and an environmentally assisted time-dependent crack growth model to predict the creep–fatigue–environment interactions in creep–brittle materials. This new model addresses the issues more comprehensively by including effects of temperature. The cycle dependent component, $(da/dN)_{cycle}$, can be divided into the athermal and the thermally activated dislocation components and the time rate of crack growth in this model is given by Eq. 30.

$$\frac{da}{dt} = \alpha \bar{A} \exp\left(-\frac{Q}{R_G T}\right) C_0 \left(\frac{4\pi\gamma^3}{3kT} \left[\frac{k^2}{tr}\right]^{\frac{1}{n+1}} \beta (\hat{\sigma}_{xx}(\theta, n) + \hat{\sigma}_{yy}(\theta, n))\right) \quad (30)$$

Equation 30 can be written as a simplified Eq. 31.

$$\frac{da}{dt} = A' \exp\left(\Psi K^{\frac{2}{1+n}}\right), \quad (31)$$

where,

$$\Psi = \Psi' \left(\frac{1}{T}\right) \left(\frac{1}{t}\right)^{\frac{1}{n+1}}, \quad (32)$$

$$A' = A'' \exp\left(-\frac{Q}{R_G T}\right) \quad (33)$$

and A' and Ψ are determined from the regression analysis, Ψ' and A'' are constants, Q is the activation energy

of the reaction, and t is the time at any point along the cycle. A comprehensive model can be obtained by combining the time and cycle dependent terms and using the definition that $K_{max} = \Delta K / (1 - R)$ to get

$$\left(\frac{da}{dN}\right)_{tot} = q \Delta K^{n_1} + c_0 \cdot \Delta K^{m_0 + \frac{c_1}{R}} \cdot \exp\left(-\frac{Q_0}{R_G T}\right) + \int_0^{t_h} A'' \exp\left(-\frac{Q}{R_G T}\right) \times \exp\left(\Psi' \left(\frac{1}{T}\right) \left(\frac{1}{t}\right)^{\frac{1}{n+1}} \frac{\Delta K}{1-R}^{\frac{2}{n+1}}\right) dt \quad (34)$$

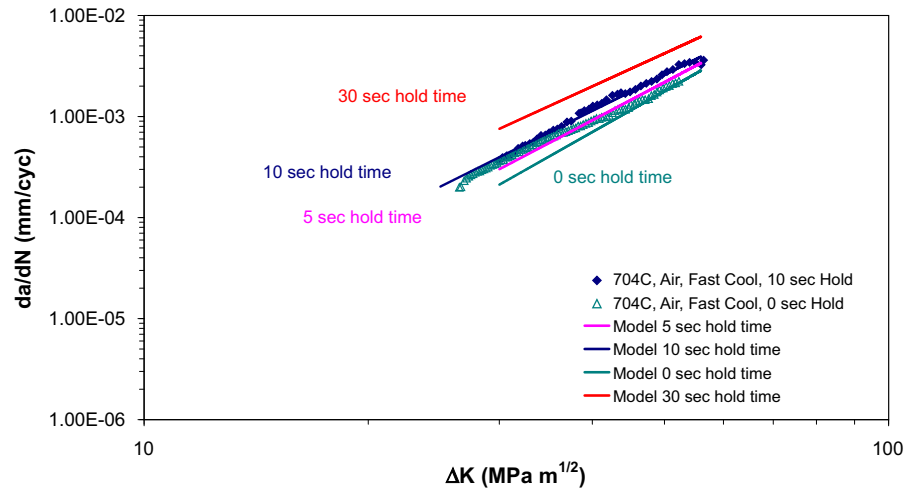
The total crack growth rate, $(da/dN)_{tot}$, can thus be determined by obtaining a curve fit for the elevated temperature fatigue crack growth rate (FCGR) data. The $(da/dN)_{ath}$ crack growth rate can be determined from regression of room temperature data and $(da/dN)_{th}$ is obtained from time and environment independent data acquired at elevated temperature by testing in vacuum. The constants for this model were determined using FCGR data obtained in air at 25 °C and in a vacuum and in air at 704 °C using a 0 and 10 s hold time for the Ni-base superalloy ME3 (Evans and Saxena 2009). For the thermally activated dislocation based crack growth rate model, the material constant m was assumed to be independent of temperature (Evans 2008). The activation energy, Q , was estimated to be 33,455 J/mol. The agreement between the model and the experimental results for 0 and 10 s is shown in Fig. 10 showing a good fit with the test data. Also, the prediction for 5 and 30 s hold times fall within the expected behavior.

Several gaps exist in understanding and modeling the creep–fatigue–environment interactions in creep–ductile and creep–brittle materials. The necessary analytical and experimental tools for such work are available and by focusing on that can raise the understanding and the related technology to the next higher level needed to design structural components that will operate under extreme environment conditions.

4 Creep and creep–fatigue behavior in welds containing mis-matched creep properties

Weld integrity is often an issue with high temperature components. However, welds present special challenges because of the complexity of microstructural gradients in the weld region where the defects are

Fig. 10 A comparison between predicted and experimental results for Ni base alloy ME3 (Evans 2008)



present and the environment in which they grow. The microstructure consists of the base metal (BM), weld metal (WM) and a heat affected zone (HAZ). Typically, the boundaries between these regions are not sharp and the surfaces not planar so crack tips can meander from one region to another as the cracks grow. The creep deformation properties may vary between the three major regions of the weld and therefore it cannot be considered homogeneous for analytical purposes, except for the elastic properties. Even while recognizing the complexities, the analytical models assume sharp interfaces and the crack to be located at the interface with different creep deformation properties on either side of the interface. For these idealized situations, it is shown that strains can preferentially accumulate in the weaker region and cause the cracks to grow in that region (Cretegnly and Saxena 1998). Further, if we assume power-law creep to be operative on either side of the interface, C^* can be shown to be path independent making it measurable using the load-line displacement rate. Even for small-scale creep, the creep zone expansion will be uneven on the two sides of the interface but its expansion rate will be measurable at the loading points. This makes C_t to be a valid parameter for characterizing the creep crack growth rate and $(C_t)_{avg}$ to be valid for creep-fatigue conditions.

Creep and creep-fatigue crack growth tests were conducted on weldments (Grover 1997) using different hold times, starting crack sizes, different material conditions such as welds with over-matched and under-matched weld materials. Fatigue crack growth tests without hold time were conducted using specimens D1 and D2 from the base material, and TC1,

TC2, and TC5 from welds at a cyclic frequency of 1 Hz, Fig. 5, showing virtually identical behavior from all specimens. This shows that if the conditions remain dominantly elastic, the fatigue crack growth behavior between the weld metal and the base metal remain similar.

The data from tests with different hold times of 10, 60, and 600 s are plotted in Fig. 11 (Grover 1997; Grover and Saxena 1999; Saxena 2007). Included in this plot are data from tests conducted on the base metal and also over-matched and under-matched weldments and the data from creep crack growth tests conducted on the base material. The $(C_t)_{avg}$ values in Fig. 11 were obtained from load-line displacements measured during the hold time, thus, it accounts for the composite creep deformation rates for the weld metals and the respective base metal. There seems to be some difference between the CCG (creep crack growth rate) and the CFCG behavior; the overmatched weld condition seems to perform slightly better under creep-fatigue conditions.

It was also noted from these studies that the differences between the $(da/dt)_{avg}$ versus $(C_t)_{avg}$ behavior between the various material conditions is small (a factor of four) compared to much larger differences in the creep deformation behavior (almost two orders of magnitude depending on the applied stress). This, however, does not imply that the different weld conditions will result in creep-fatigue lives that are within a factor of four of each other. On the contrary, the differences can be quite large because the higher creep rates in welds that are less resistant to creep deformation will yield higher $(C_t)_{avg}$ compared to the ones that are more

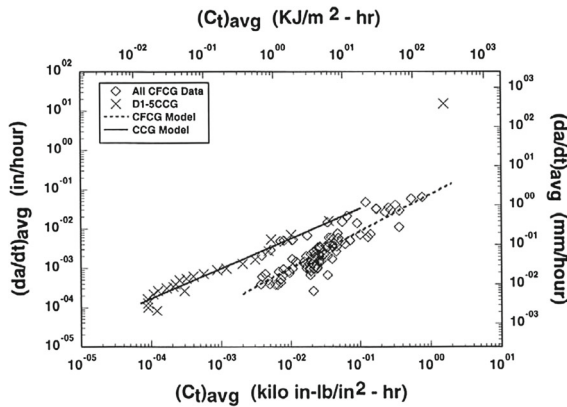
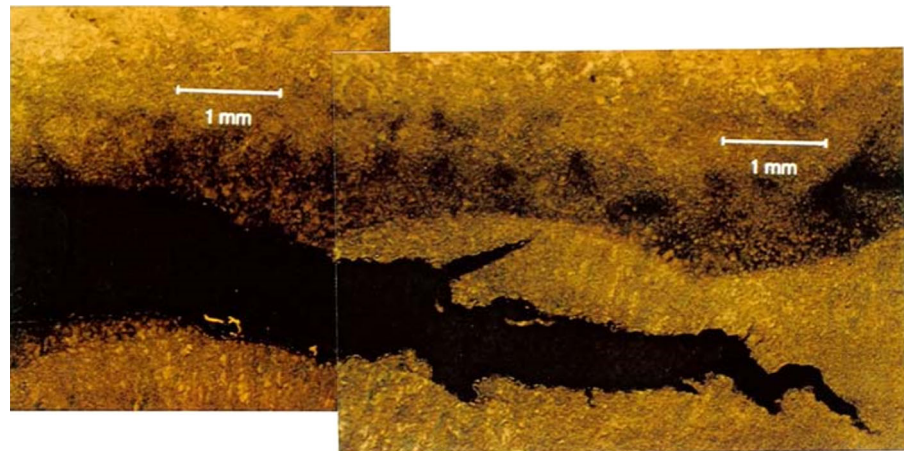


Fig. 11 Creep–fatigue crack growth data from base metal, under-matched welds and over-matched welds and creep crack growth data from the base material in weldments from a Cr–Mo–V steel. All tests were conducted at 565 °C (Grover 1997; Grover and Saxena 1999; Saxena 2007)

resistant to creep deformation at equal load levels and will result in much shorter lives. Calculating $(C_t)_{avg}$ from the measured load-line displacements normalizes the effects of higher creep deformation rates and tends to consolidate the CCG and CFCG data into a much closer band.

Figures 12 and 13 show the crack path of various CFCG specimens from welds. Figure 12 shows the crack path followed by a CFCG specimen from an under-matched weld TC1 and the crack appears to first follow the fusion line and then it turns into the WM, as would be expected because the WM creep rates are significantly higher (68 times at 207 MPa stress level) than the BM creep rates. The $(da/dt)_{avg}$ versus $(C_t)_{avg}$ behavior was higher for this condition than for the others. Figure 13 shows the crack path of a CFCG spec-

Fig. 12 Fracture path of a CFCG specimen from the under-matched weldment TC1 showing a crack path along the fusion line and in the weld metal region (Grover 1997; Saxena 2007)

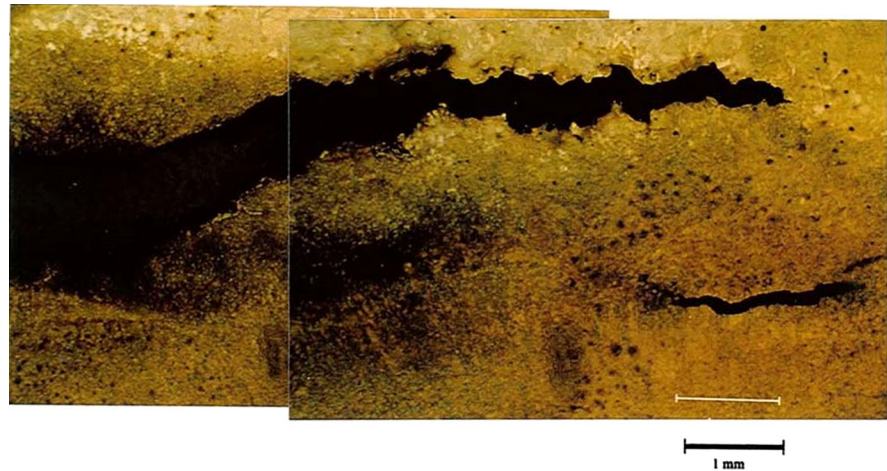


imen from the overmatched weldment TC5 in which the crack path meanders from the fusion line into the BM which is the less creep resistant constituent in this weldment.

The justification for using time-dependent fracture mechanics for addressing crack growth in weldments utilizes a basic representation of weldments consisting of a bimaterial with a sharp crack located along the fusion line subjected to a load normal to the fusion line. This simple picture results from the fact that the J -Integral, and the C^* -Integral are both path-independent for such a configuration under elastic-plastic and dominantly secondary creep conditions, respectively (Shih and Asaro 1988; Asaro and Shih 1989; Asaro et al. 1993; Shih 1991; Nakagaki et al. 1991). This assures the uniqueness between the crack tip stress fields and the magnitude of the crack tip parameter(s) and the ability to measure their magnitudes at the loading pins. This model predicts that there is strain intensification in the material that has lower resistance to deformation with the implication that there is greater potential for cracks to grow on that side of the interface. This general statement has been proven to be right by the data that is presented above (Saxena 2007; Cretegnny and Saxena 1998). Thus, fracture mechanics has a definite role in representing crack growth in weldments. It is thus necessary to also understand the limitations of this approach that will require the following additional work.

Finite element studies should be carried out to explore a number of factors that influence the growth of cracks by creep and fatigue in weldments subjected to high temperatures. An understanding of the evolution of the crack tip fields and the balance of driving

Fig. 13 Fracture path in a CFCG specimen from an overmatched weldment TC5 showing crack path along the BM/HAZ interface region and then meandering into the base metal (Grover 1997; Saxena 2007)



and resisting forces for cracks is fundamental to any fracture analysis. Nonlinear and time-dependent finite element analyses must be performed to investigate the crack tip stress fields as a function of time when a mismatch of creep properties exists at the interface. Analysis must initially focus on stationary cracks located at various distances from the weld fusion-line subjected to static and cyclic loading of the type encountered during service. Creep conditions spanning small-scale creep to extensive creep regimes must be examined. Consideration must be given to constitutive laws which account for combinations of elastic, plastic, primary creep, and secondary creep deformation, as appropriate for the system being modelled. The results of the simulations must be used to develop simple expressions for estimating the magnitudes of crack tip parameters for engineering components.

The analyses must treat the material on both sides of the interface as inelastic and deformable. Cracked configurations with identical elastic properties but different creep and plastic properties with due consideration to the microstructural gradients across the fusion line must be examined. Comparison of crack tip fields with those resulting in homogeneous bodies will reveal the trends that develop as the mismatch increases and the property gradients intensify. Solutions must be obtained for both stationary and growing cracks. The thickness of the interface layer and the property gradients must be systematically varied in some parametric form, along with crack position in the interface layer, crack length and crack path.

The effect of graded interfaces on the transition from small-scale creep to extensive creep must be examined.

The relationship between global stress-power release rate with crack size to near tip values including their relationships to crack tip creep zone evolution must be examined to assess the limitations of global parameters for correlating creep and creep–fatigue crack growth rates. The analysis must also attempt to model cyclic loading conditions to understand the development of cyclic plasticity at the crack tip and its subsequent effect on the evolution of the creep fields during hold time.

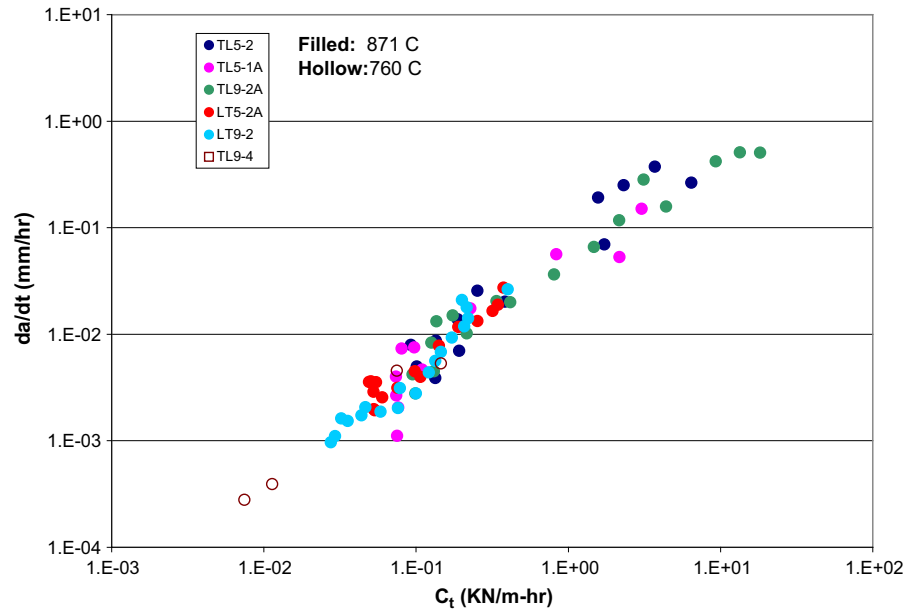
5 Creep and creep–fatigue crack growth test methods

5.1 Creep crack growth test methods

The experimental methods for measuring creep crack growth rates have been standardized in an American Society for Testing and Materials (ASTM) standard (ASTM Standard E1457-07 2007). Thus, for long-term sustained loading conditions, the fracture mechanics methods for characterizing creep crack growth rates are reasonably well established. Areas that need further development are discussed briefly.

- In creep-brittle materials, considerable amount of crack extension both in specimens and in components can occur under transient conditions. The approaches for characterizing the crack growth rate under such transient conditions are not adequately established.
- The specimens recommended for testing in the standard E1457 represent a variety with different

Fig. 14 Creep crack growth behavior of DS-GTD 111 at different temperatures for specimens machined such that the loading direction was in the direction of the grains (LT) and transverse to the direction of the grains (TL) (Ibanez et al. 2006a). The data also includes tests conducted at different temperatures



levels of constraint. The effects of crack tip constraint on the creep crack growth behavior has not been systematically investigated so there is concern about the equivalency of creep crack growth behavior obtained from various geometries with high and low constraints.

- The deformation based global fracture mechanics parameters are only valid when creep cavitation damage is limited to a small region in the vicinity of a crack. If the damage is widespread, other approaches based on damage mechanics are more appropriate. The limits on the use of fracture mechanics have not been systematically studied.
- Several high temperature materials in gas turbine applications are single crystal or directionally solidified materials with strong directional characteristics. This problem has barely been addressed. The correlation between da/dt and C_t for directionally solidified GTD-111 Ni-based alloy is shown in Fig. 14 (Ibanez et al. 2006a, b) for tests conducted on specimens machined from different orientations. Limited finite element simulations of such tests have also been conducted (Gardner et al. 2001; Ma et al. 2014). More experiments as well as simulations should be conducted to enhance our understanding of DS and single crystal materials.
- There are some guidelines in ASTM E1457 for testing weldments but there are still major gaps in the understanding of how to conduct the tests that are

more meaningful in replicating service conditions. Considering the importance of welds in high temperature components, this topic has not received the attention it deserves.

5.2 Creep–fatigue crack growth test methods

ASTM Standard E2760-10 (2010) addresses the standard method for characterizing the creep–fatigue crack growth behavior. Areas of advancement of these methods include the following.

- The Standard E2760 restricts creep–fatigue crack growth tests to only one specimen geometry and only under conditions of load-control. The amount of crack extension in the specimens that is considered valid is limited by ratcheting in the specimens with cycles. Additional specimen geometries and displacement-controlled tests should be introduced in the standard method so the range of valid crack growth data can be extended to deeper crack sizes making better use of the specimens' capability to measure crack growth.
- Advancements are needed to more accurately measure changes in load-line displacement during the hold time and also the increases in crack size during the hold period to enhance our understanding of the creep–fatigue interactions.

- The interrelationships between the various damage mechanisms that operate under the severe service conditions are complex. Thus, the development of physics-based models for predicting design or remaining life must be guided by experimental studies that are specifically aimed at fundamental understanding of these mechanisms. These experiments are challenging and demand precise environmental control capability, extremely high resolution in the measurement of displacements associated with creep strains and also in measurements of crack increments at high temperatures such as during hold time. Recent advancements in analytical, experimental and computational techniques can be used in concert to enable very significant advances in our understanding of these component life-limiting considerations that are currently not fully understood.

6 Applications

The performance of high temperature components such as natural gas-fired turbines, aircraft turbines and steam turbines has steadily improved with the continuous development of advanced materials and design concepts. Since these materials are being pushed to the limits of their capability, accurate mathematical models such as ones described in the earlier sections of this paper are needed to predict the life of high temperature components to prevent unscheduled outages due to sudden failures. There is also a need to develop realistic inspection intervals and criteria to avoid sudden failures but they must not be too conservative because of operational cost considerations.

Figure 15 shows a schematic diagram of all elements of a methodology for prognostics of high temperature component reliability that includes the use of constitutive equations, crack formation and crack growth models under high temperature conditions (Saxena 2013). The models must be able to account for complex conditions consisting of low frequency cyclic stress associated with thermal and mechanical loads generated during startup and shutdown, sustained stress resulting from centrifugal loading and aerodynamic loads during steady-state operation leading to creep conditions, and damage phenomena in high temperature materials under conditions of creep, oxidation, fatigue, and the synergistic effects of creep–fatigue–oxidation. The

goal for technologies used for assessing reliability of hot gas path parts in industrial and aircraft turbines and steam turbines must be to realistically estimate:

- Frequency and extent of required inspections during outages and the criteria for run, repair, retire, decisions,
- The level of online monitoring needed to update the prognostics of reliability in the face of changing operating conditions from those used to design the components,
- Establishing better and more realistic process control and inspection criteria for acceptance of critical components,
- Avoiding unexpected outages and reducing maintenance costs and,
- Deriving the full useful life from capital intensive equipment and components.

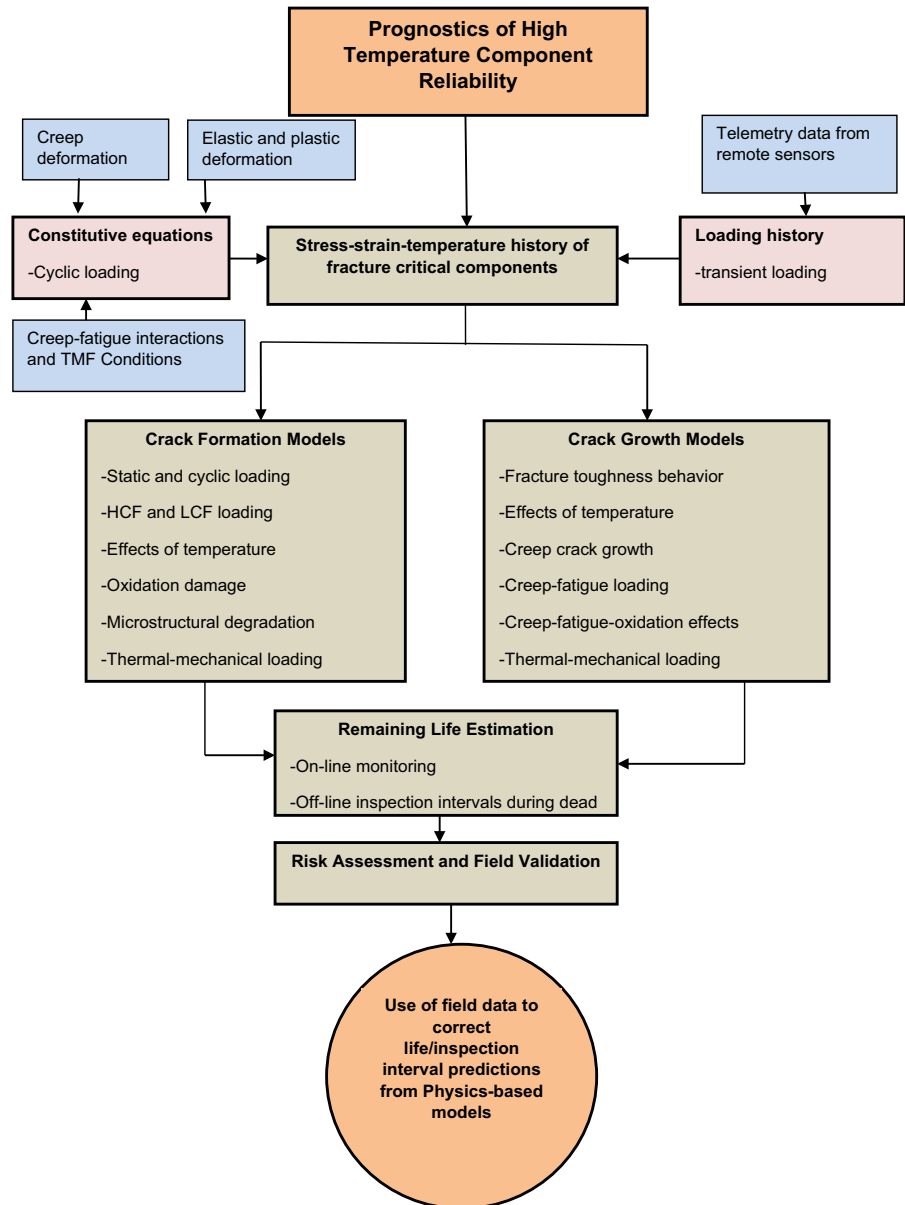
Due to advances in online sensors, better service and maintenance records and the availability of operating data during service, including results from the prior non-destructive inspections, more reliable estimates of remaining life of high temperature components are possible that are individualized to specific components based on their specific loading history. These predictions can replace the need to make generalized recommendations that apply to whole fleet of components that by nature must be conservative. In that context it is essential that all this service data be used to improve the prognostics of high temperature components to reduce the uncertainty in lives as called for in Fig. 15. Use of expert systems for such applications must be developed.

7 Summary, conclusions and recommendations for future work

This paper presents the progress made in the field of time-dependent fracture mechanics to account for creep deformation at the crack tip at elevated temperatures. The following bullets outline the progress that has been made and the future work that must be undertaken to develop the technology further in this age where information gathering and retrieval has become a lot easier and it can be used to customize the prediction of life of specific components.

Analytical frame-work exists for predicting creep and creep–fatigue crack growth in creep-ductile materials and to lesser degree for creep-brittle materials

Fig. 15 A methodology for prognostics of high temperature component reliability



and DS materials. Additional work is needed to understand the transients due to the effects of growing cracks and the development of creep deformations in front of a moving crack tip. For DS materials, we need to account for grain boundaries and difference in crystallographic orientations on the creep deformation at the crack tip as the crack transitions from one grain to the next

- Advancements are needed in efficiently collecting crack growth data during creep–fatigue tests; in par-

ticular displacement controlled test methods should be explored.

- Models for predicting the effects of creep and environment are presented in the paper. However, more fundamental studies are needed to better understand creep–fatigue–environment interactions.
- Significant effort should be devoted to the application of the currently available models in a frame-work of risk assessment in conjunction with on-line and off-line damage monitoring and inspection data. Field validation of creep–fatigue

model predictions should be given a very high priority.

- Some progress has been made in the assessment of crack growth in welds under creep–fatigue. Future studies must consider;
 - Microstructural gradients and transition layers between the weld metal and the base metal,
 - Sharp interfaces, though useful for qualitative judgments, are not always realistic,
 - Plastic and creep deformation zones and their evolution in the welds, including their interaction with the transition layer must be studied in detail to understand the limitations of nonlinear fracture mechanics to problems of mismatched welds,
 - Analytical crack growth studies performed should model cracks that meander from one region of the weld to another to develop robust models.

Acknowledgments The author is deeply indebted to several of his present and past collaborators for their insightful discussions and their work that have directly and indirectly contributed to the research described in this paper. Particularly noteworthy are the contributions of Drs. R. Viswanathan, David L. McDowell, Bilal Dogan, Stephen D. Antolovich, Hugo Ernst, John D. Landes, James A. Begley, John Bassani, Herbert Hui, Herman Riedel, and K. Yagi. His former PhD students and Post-docs whose contributions are invaluable include C.P. Leung, Brian Gieseke, Kee Bong Yoon, Negussie Adefris, Richard H. Norris, Yancy Gill, Parmeet Grover, David Hall, B. Carter Hamilton, Jeffery Evans, Kip Findley, Heather Major, Alejandro Ibanez, Jidong Kang, Bruce Antolovich, Sau-wee Koh, V. Kalyanasundaram, Santosh Narasimhachary, and V. Srinivasan. The financial support of this work was provided by the Electric Power Research Institute, the National Science Foundation, and by several companies. The support from the George and Boyce Billingsley Endowed Chair at the University of Arkansas is also gratefully acknowledged.

Open Access This article is distributed under the terms of the Creative Commons Attribution License which permits any use, distribution, and reproduction in any medium, provided the original author(s) and the source are credited.

References

- Asaro RJ, O'Dowd NP, Shih CF (1993) Elastic plastic analysis of cracks in bimaterial interfaces: interfaces with structure. *Mater Sci Eng A* 162:175–192
- Asaro RJ, Shih CF (1989) Elastic-plastic analysis of cracks on bimaterial interfaces: part II—structure of small-scale yielding fields. *J Appl Mech* 56:763–779
- ASTM Standard E1457-07 (2007) Standard test method for measurement of creep crack growth rates in metals (1992). ASTM Book of Standards, American Society for Testing and Materials, Philadelphia
- ASTM Standard E2760-10 (2010) Standard test method for measurement of creep–fatigue crack growth. ASTM Book of Standards, American Society for Testing and Materials, Philadelphia
- Bassani JL, Hawk DE, Saxena A (1989) Evaluation of C_t parameter for characterizing creep crack growth rate in the transient regime. In: *Nonlinear fracture mechanics: time-dependent fracture mechanics*, ASTM STP 995. American Society for Testing and Materials, Philadelphia
- Bassani JL, McClintock FL (1981) Creep relaxation of stress around a crack tip. *Int J Solids Struct* 17:79–89
- Cretegy L, Saxena A (1998) Fracture toughness behavior of weldments with mis-matched properties at elevated temperature. *Int J Fract* 92:119–130
- Evans JL (2008) Environment assisted crack growth in Ni-base superalloys at elevated temperature, PhD Dissertation. College of Engineering, University of Arkansas, Fayetteville, AR
- Evans JL, Saxena A (2009) Elevated temperature crack growth rate model for Ni-base superalloys. In: *Proceedings of the 12th international conference on fracture*, Ottawa, Canada
- Floreen S, Kane RH (1980) An investigation of creep–fatigue–environment interactions in Ni base superalloys. *Fatigue Eng Mater Struct* 2:401–412
- Gardner B, Qu J, Saxena A (2001) Creep crack growth parameters for directionally solidified superalloys. In: *Proceedings of the tenth international conference on fracture*, Honolulu, Hawaii
- Grover PS (1997) Creep–fatigue crack growth in Cr–Mo–V base material and weldments. PhD Dissertation, Georgia Institute of Technology, Atlanta, GA
- Grover PS, Saxena A (1995) Characterization of creep–fatigue behavior in 2.25Cr–1Mo steel using $(C_t)_{avg}$ parameter. *Int J Fract* 73:273–286
- Grover PS, Saxena A (1999) Modeling the effect of creep–fatigue interaction on crack growth. *Fatigue Fract Eng Mater Struct* 22:111–122
- Hall DE, Hamilton BC, McDowell DL, Saxena A (1997) Creep crack growth behavior of aluminum alloy 2519: part II numerical analysis. In: *Effects of temperature on fatigue and fracture*. ASTM STP 1297, pp 19–36
- Hamilton BC, Hall DE, Saxena A, McDowell DL (1997) Creep crack growth behavior of aluminum alloy 2519: part I—experiments. In: *Effects of temperature on fatigue and fracture*, ASTM STP 1297. American Society for Testing and Materials, pp 3–18
- Hutchinson JW (1968) Plastic stress and strain fields at a crack tip. *J Mech Phys Solids* 16:13–31
- Hui CY (1983) Steady-state crack growth in elastic power-law creeping material. In: *Elastic–plastic fracture*, ASTM STP 803, vol I. American Society for Testing and Materials, Philadelphia, pp 573–593
- Hui CY (1986) The mechanics of self-similar crack growth in elastic power-law creeping material. *Int J Solids Struct* 22:357–372

- Hui CY, Riedel H (1981) The asymptotic stress and strain field near the tip of a growing crack under creep conditions. *Int J Fract* 17(4):409–425
- Ibanez A, Saxena A, Kang J (2006) Creep behavior of directionally solidified nickel based superalloy. *J Strength Fract Complex* 4(2006):75–81
- Ibanez A, Srinivasan VS, Saxena A (2006b) Creep deformation and rupture behavior of directionally solidified GTD 111 superalloy. *Fatigue Fract Eng Mater Struct* 29:1010–1020
- James LA (1972) The effect of frequency upon the fatigue crack growth of type 304 stainless steel at 1,000 °F. In: *Stress analysis and growth of cracks*, ASTM STP 513. American Society for Testing and Materials, Philadelphia, pp 218–229
- Kumar V, German MD, Shih CF (1981) *An engineering approach for elastic–plastic analysis*, EPRI Report NP-1931. Electric Power Research Institute, Palo Alto, CA
- Landes JD, Begley JA (1976) A fracture mechanics approach to creep crack growth. In: *Mechanics of crack growth*, ASTM STP 590. American Society for Testing and Materials, Philadelphia, pp 128–148
- Ma YW, Yoon KB, Saxena A (2014) Evaluation of creep crack growth for directionally solidified Ni-base superalloy using a newly proposed anisotropic estimation scheme for C_t equation. In: *Symposium on HTMTC creep–fatigue crack development EMPA Dübendorf, Switzerland*
- Nakagaki M, Marshall CW, Brust FW (1991) Elastic–plastic fracture mechanics evaluations of stainless steel tungsten/inert gas welds. In: *Fracture mechanics: elastic–plastic fracture, vol II*. American Society for Testing and Materials, ASTM STP 995, pp 214–243
- Narasimhachary SB, Saxena A (2013) Crack growth behavior of 9Cr–1Mo steel under creep–fatigue conditions. *Int J Fatigue* 56:106–113
- Nikbin KM, Webster GA, Turner CE (1976) Relevance of nonlinear fracture mechanics to creep crack growth. In: *Crack and fracture*, ASTM 601. American Society for Testing and Materials, Philadelphia, pp 47–62
- Ohji K, Ogura K, Kubo S (1979) Stress-strain fields and modified J-integral in the vicinity of the crack tip under transient creep conditions. *Jpn Soc Mech Eng* 790(13):18–20 (in Japanese)
- Pelloux RM, Huang JS (1980) Creep–fatigue–environment interactions in astroloy. In: Pelloux R, Stoloff NS (eds) *Creep–fatigue–environment interactions*. TMS-AIME publishers, Warrendale, PA, pp 151–164
- Rice JR (1968) A path-Independent integral and the approximate analysis of strain concentration by notches and cracks. *J Appl Mech Trans ASME* 35:379–386
- Rice JR, Rosengren GF (1968) Plane strain deformation near a crack tip in a power-law hardening material. *J Mech Phys Solids* 16:1–12
- Riedel H (1981) Creep deformation of crack tips in elastic–viscoplastic solids. *J Mech Phys Solids* 29:35–49
- Riedel H (1983) Crack tip stress fields and crack growth under creep–fatigue conditions, elastic–plastic fracture. In: *Second symposium. Inelastic analysis*, ASTM STP 803, vol I. American Society for Testing and Materials, Philadelphia, pp I/505–I/520
- Riedel H, Rice JR (1980) Tensile cracks in creeping solids. In: *Twelfth conference*, ASTM STP 700. American Society for Testing and Materials, Philadelphia, pp 112–130
- Reidel H, Wagner W (1981) The growth of macroscopic cracks in creeping materials. In: *advances in fracture research*. Pergamon Press, Oxford
- Saxena A (1980) Evaluation of C^* for characterization of creep crack growth behavior of 304 stainless steel. In: *Fracture mechanics: twelfth conference*, ASTM STP 700. American Society for Testing and Materials, Philadelphia, pp 131–151
- Saxena A (1983) A model for predicting the environment enhanced fatigue crack growth behavior at high temperatures. In: *Thermal and environment effects in fatigue: research design interface*, PVP, vol 71. American Society for Mechanical Engineers, pp 171–184
- Saxena A (1986) Creep crack growth under non steady state conditions. In: *Fracture mechanics: seventeenth volume*, ASTM STP 905. American Society for Testing and Materials, Philadelphia, pp 185–201
- Saxena A (1998) *Nonlinear fracture mechanics for engineers*. CRC Press, 472 p, ISBN 0-8493-9496-1
- Saxena A (2007) Role of nonlinear fracture mechanics in assessing fracture and crack growth in welds. *Eng Fract Mech* 74:821–838
- Saxena A, Bassani JL (1984) Time-dependent fatigue crack growth behavior at elevated temperature, fracture. In: *Interactions of microstructure, mechanisms and mechanics*. TMS-AIME, Warrendale, PA, pp 357–383
- Saxena A, Ernst HA, Landes JD (1983) Creep crack growth behavior in 316 stainless steel at 594 °C. *Int J Fract* 23:245–257
- Saxena A, Gieseke B (1987) Transients in elevated temperature crack growth. In: *Proceedings of MECAMAT, international seminar on high temperature fracture mechanisms and mechanics III*, EGF-6, pp 19–36
- Saxena A, Liaw PK, Logsdon WA (1986) Residual life prediction and retirement for cause criteria for SSTG upper casings. Part II. *Fract Mech Anal Eng Fract Mech* 25:289–303
- Saxena A, Narasimhachary SB, Kalyanasundaram V (2013) Prognostics of high temperature component reliability. In: *Thirteenth international conference on fracture*, Beijing
- Saxena A, Williams RS, Shih TT (1981) A model for representing and predicting the influence of hold time on fatigue crack growth behavior at elevated temperature. In: *Fracture mechanics: thirteenth conference*, ASTM STP 743. American Society for Testing and Materials, Philadelphia, pp 86–99
- Saxena A, Yagi K, Tabuchi M (1994) Creep crack growth under small scale and transition creep conditions in creep-ductile materials. In: *Fracture mechanics: twenty fourth volume*, ASTM STP 1207. American Society for Testing and Materials, Philadelphia, pp 481–497
- Shih CF (1991) Cracks in bimaterial interfaces: elasticity and plasticity aspects. *Mater Sci Eng A* 143:77–90
- Shih CF, Asaro RJ (1988) Elastic–plastic analysis of cracks on bimaterial interfaces: part I—small-scale yielding. *J Appl Mech* 56:299–316
- Siverns MJ, Price AT (1973) Crack propagation under creep conditions in quenched $2\frac{1}{4}$ Cr–1Mo steel. *Int J Fract* 9:199–207
- Taira S, Ohtani R, Kitamura T (1979) Application of J-integral to high temperature crack propagation: part I—creep crack propagation. *J Eng Mater Technol* 101:154–161

- Yokobori T, Yokobori AT, Kamei A (1975) Dislocations dynamics theory for fatigue crack growth. *Int J Fract* 11:781–788
- Yoon KB, Saxena A, Liaw PK (1993) Characterization of creep-fatigue crack growth behavior under trapezoidal wave shape using C_t parameter. *Int J Fract* 59:95–114
- Yoon KB, Saxena A, McDowell DL (1992) Influence of crack tip plasticity on creep-fatigue crack growth. In: *Fracture mechanics: twenty second symposium*, ASTM STP 1137, vol 1. American Society for Testing and Materials, Philadelphia, pp 367–392